Proceedings of the 11th ICPMG 2026
11th International Conference on Physical Modelling in Geotechnics
8-12 June 2026, Zurich, Switzerland

Centrifuge model tests on failure mechanism of dual structure slope under gradual excavation condition

Y.Y. Hao, G. Zhang
Tsinghua University, Beijing, China, haoyueyan0824@gmail.com, zhangga@tsinghua.edu.cn

ABSTRACT: Gradual slope excavation is a common engineering practice, but it carries significant instability risks. Most previous researches have put their focus on homogeneous slopes, while natural slopes are often heterogeneous. Therefore, studying the failure mechanism of heterogeneous slopes under gradual excavation is crucial. In this study, excavation centrifuge model tests are conducted on both a heterogeneous slope model containing clay and sand and a homogeneous one with clay as control. In the tests, excavation was performed in five steps, and an image-based measurement system is used to capture full-field displacement history of the slopes during the tests. The results show that the slopes both have a part with similar range occurring rapid failure during excavation. The dual structure slope landslides at excavation depth of 150mm while failure in the pure clay one appears when excavation depth is 120mm. in a similar range during gradual excavation. The two slopes share similar failure mechanism which can be explained by the coupling effect of deformation localization and local failure. Dual structure significantly affects the slope's response under excavation. It brings difference in deformation distribution and therefore changes the slip surface pattern and location. The dual structure also alters the slope failure process by slowing the rate of deformation development and enhancing the slope's bearing capacity against excavation, while at the same time reducing its resistance to deformation localization.

1 INTRODUCTION

Gradual slope excavation is widely adopted in engineering practices such as roads and tunnels construction (Zhang et al., 2019; Paudyal et al., 2023). However, repeated excavation progressively reduces slope stability and may trigger landslides or collapses (Zhang et al., 2012). Natural slopes are often heterogeneous, among which the dual-structure type is a representative example. It has been revealed that interactions within different structural components can lead to distinct failure behaviors in dual structure slopes. However, despite existing numerical studies can quantify stress–displacement responses and assess slope stability through safety factors, understanding the evolution of deformation and failure mechanisms in heterogeneous slopes under excavation remains a challenging problem (Yang et al., 2019; Gao et al., 2022).

Centrifuge model testing offers a powerful experimental approach in simulating realistic stress field, boundary effects, and continuously observing slope deformation and failure. In-flight excavation techniques have been developed, enabling investigation of factors such as slope geometry and excavation height (Li et al., 2011). By integrating centrifuge observations with triaxial test results, the progressive retreat failure mechanism of loess slopes during excavation has been clarified (Zhang et al., 2020). In addition, the instability mechanisms of slopes subjected to coupled effects—such as excavation combined with water-level fluctuations or structural reinforcement—have also been examined (Huang et al., 2023; Liu et al., 2024).

However, previous centrifuge model studies mainly focus on homogeneous slopes and pay limited attention to the influence of structural heterogeneity. Therefore, it is necessary to carry out centrifuge model tests on dual-structure slopes under gradual excavation conditions to clarify how heterogeneity affects slope stability and failure mechanisms.

In this study, a dual-structure slope composed of sand and clay is modeled, with a pure clay slope used for comparison. Centrifuge model tests are performed with in-flight gradual excavation. The full-field displacement of both slopes is measured, and the deformation and failure mechanisms, including the effects of dual structure, are analyzed.

2 TESTS

2.1 Test program

The slope model with two layers containing clay and sand is employed to analyse the failure mechanism of dual structural slopes during gradual excavation while a pure clay model of identical geometry is chosen as control. Centrifuge model testing is adopted as the primary research method. After the excavation device is installed, multiple excavation stages can be performed on each model during centrifuge operation. The deformation and failure processes of both the dual-structure and pure clay slopes are subsequently simulated and analyzed.

2.2 Model

Both slope models have a gradient of 0.8:1 and a height of 280 mm. Figure 1 illustrates the configuration of the dual structure slope, consisting of two horizontal layers. The upper and lower layers are composed of sand and clay, respectively, each with a thickness of 140 mm. The size and shape of the pure clay slope are the same as the dual structure one but contains only clay without layering.

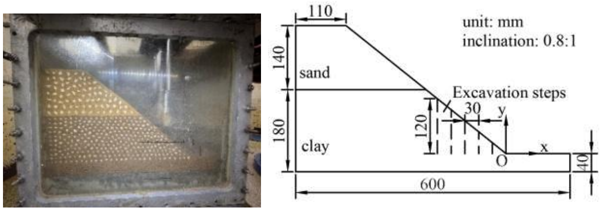

(a) (b)

Figure 1. Slope models. (a) photo of the dual structure slope in model box; (b) structural diagram of the dual structure slope.

During model preparation, soil was premixed with water to reach target water content and compacted layer by layer within the model container to the specified density, with each layer 40 mm thick. An additional 40 mm-thick foundation of the same material was placed at the bottom of the model box to minimize the influence of contact with the container. The surface of each layer was scraped to enhance bonding with the overlying layer. The slope geometry was then carved after all layers are completed.

To better reflect the differences and interactions between layers in the dual-structure slope, sand and clay were selected because of their contrasting strength and deformation characteristics. The sand used in the tests was Fujian standard sand, with the water content of 17% and density of 1.6 g/cm^3 and.Its average soil particle size, d_{60} and d_{10} were 0.45mm, 0.5mm and 0.29mm, respectively. The clay was a silty clay with the water content of 17% and density of 1.6 g/cm^3. Its liquid and plastic limits are 31% and 17%, respectively.

2.3 Equipment

The geotechnical centrifuge at Tsinghua University was employed for the tests, with a maximum acceleration capacity of 250 g. The slope models were placed in a rigid model box measuring 600 mm in length, 200 mm in width, and 500 mm in height, which was securely mounted on the centrifuge platform. For deformation observation, a 40 mm-thick plexiglass window was installed on one side of the model box, and a high-resolution camera was positioned in front of it to capture real-time images during centrifuge operation. The recorded images were transmitted to the control room for continuous monitoring and analysis.

To perform gradual excavation under centrifugal conditions, an excavation simulator was installed on top of the model box. The structure and working principle of this device are described in detail by Li et al. (2011) (Figure 2). During testing, the simulator was remotely controlled to conduct excavation at designated positions, enabling precise simulation of staged slope excavation in flight.

(a) (b)

Figure 2. Excavation device. (a) front view; (b) top view.

2.4 Measurement

The images transmitted by the camera were recorded as time-indexed image series. Using a correlation-based image analysis algorithm with a measurement accuracy of 0.03 mm at model scale (Zhang et al., 2009), the displacement of selected points on the slope surface was obtained. During model preparation, small irregular foam fragments were attached to the slope surface near the plexiglass using pins to enhance grayscale contrast, thereby ensuring reliable performance of the correlation algorithm.

A Cartesian coordinate system was established with the origin at slope toe and the positive x and y axis directions as rightward and upward (Figure 1. (b)) Displacement is positive when moving horizontally to the right and vertically downwards. Based on the similarity law of centrifuge model test, the size and displacement in the model can be transformed to the prototype scale by multiplying acceleration. Stress and strain in the model and prototype scale are equal. Time in the prototype equals that in the model scale multiplied by the square of acceleration. All measurement results in this paper are in the model scale.

2.5 Test procedure

Both tests were carried out following the steps below:

(1) Model preparation and equipment installation. The model was prepared, and all testing devices were installed. The designated horizontal excavation positions were marked on the plexiglass panel.

(2) Centrifuge spin-up. The centrifugal acceleration was increased in increments of 10 g until reaching 50 g. After each increment, the acceleration was held constant for a period to allow the slope to reach a stable settlement condition.

(3) Staged excavation. The slope was excavated step by step until failure occurred. The excavation depth for each stage was 30 mm. During each excavation step, the blade first moved to the predetermined horizontal position, then penetrated vertically downward into the slope. After reaching the base of the slope, the blade advanced horizontally to the right to remove the soil and complete the excavation.

3 OBSERVATION

3.1 Slip surface

During gradual excavation, the dual structure slope landslides at the fifth excavation step, whereas for the pure clay slope failure occurs at the fourth one. Based on the displacement measurements of numerous points across the entire slope, slip surfaces were identified as the boundaries separating zones of significant displacement from those with minimal movement (Figure 3).

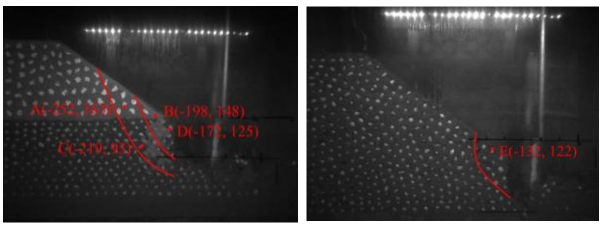

(a) *(b)*

Figure 3. Slip surface and typical points location. (a) dual structure slope; (b) pure clay slope.

In the dual structure slope, two slip surfaces developed, both intersecting the sand and clay layers. Relative displacement first occurrs along the deeper slip surface, while the final landslide took place along the shallower one. In contrast, the pure clay slope developed a single slip surface, with a longitudinal extent and height comparable to the shallower slip surface observed in the dual structure slope.

The slip surface in clay layer is like a circular arc while that in sand layer is nearly straight. This means that the clay layer slides rotationally and the sand layer experienced translationally slide. Moreover, the slip surface in the clay layer of the dual-structure slope has a smaller curvature than that in the pure clay slope, suggesting the presence of interlayer interaction.

3.2 Deformation reaction

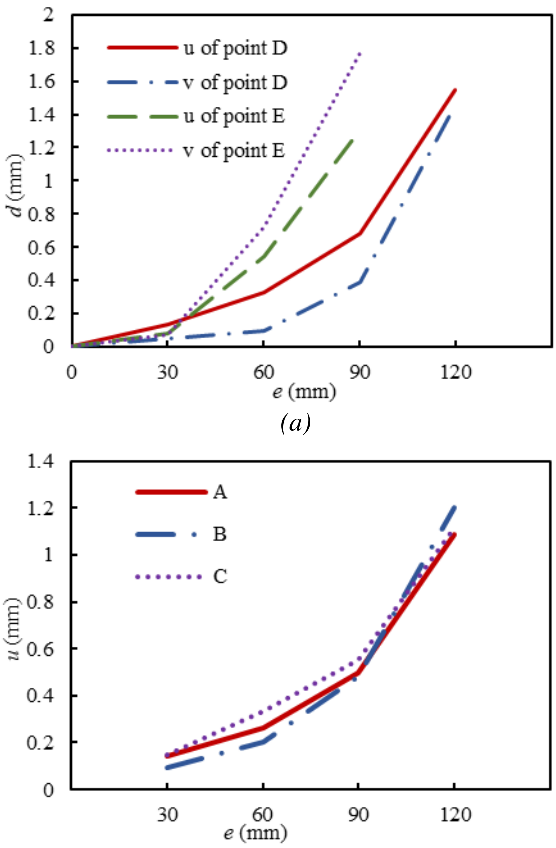

(b)

Figure 4. Displacement of typical points in figure 3 at each excavation step before failure, e, excavation depth; (x, y) point coordinates. (a) Comparation between the typical points on the sliding of clay layer in the two slopes; d, displacement. (b) horizontal displacement of three other typical points on the dual structure slope; u horizontal displacement.

The slopes cumulate deformation in each excavation steps and eventually reach failure. To show their deformation reaction due to excavation, five typical points are selected to measure displacement. Four of them distributes on each layer and above each slip surface in the dual structure slope. One of them locates in the failure part of pure clay slope. The specific locations and coordinates of the typical points are annotated in Figure 3.

Figure 4 presents the displacement of the typical points at each excavation step prior to failure. Overall, the displacement increases progressively with excavation depth, and the increment induced by each successive excavation step becomes larger than that of the previous one. The displacement in the dual-structure slope is consistently smaller than that in the pure clay slope. For example, at an excavation depth of 120 mm, the displacement in the dual-structure slope is only comparable to that at 90 mm in the pure clay slope (Figure 4(a)). This indicates that the dual-structure slope undergoes slower deformation development during excavation, which explains its later onset of failure. Moreover, the displacements of all monitored points in the dual-structure slope remain nearly identical during the first four excavation steps, regardless of the layer on which they are located or whether they eventually participate in the final failure (Figure 4(b)). This demonstrates that, before the final excavation step, the deformation within the slope is not only small but also spatially uniform across different regions.

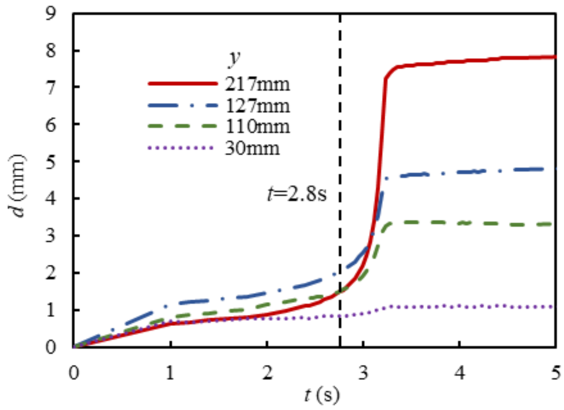

Figure 5. Relative displacement history of point couples along the deeper slip surface of the dual structure slope; y, elevation of the point pairs; t, time after the last excavation step.

The dual-structure slope first shows a tendency to slide along the deeper slip surface at the fifth excavation step. To investigate the sliding behavior at this stage, four pairs of points were selected, each pair consisting of two points located on opposite sides of the slip surface with a spacing of 10 mm. Figure 5 shows relative displacement history of the point pairs in the tangential direction of the slip surface. The tangential relative displacements increase slowly at the beginning of the fifth excavation step, followed by a sudden rise at 2.8 s. This indicates that the slide along the deeper slip surface is dominated by the uneven tangential relative there. However, shortly after the increase, the relative displacement stabilizes without further growth, explaining why final failure does not occur along the deeper slip surface.

In the final excavation step, the displacement of the typical point in pure clay slope and the two in dual structure slope above the shallower slip surface exhibit sharp and abrupt displacement surges, demonstrating that excavation induces a sudden failure in these areas (Figure 6, 7). Following this rapid failure, only limited progressive displacement is observed, suggesting that the deformation process is dominated by the instantaneous collapse rather than gradual movement.

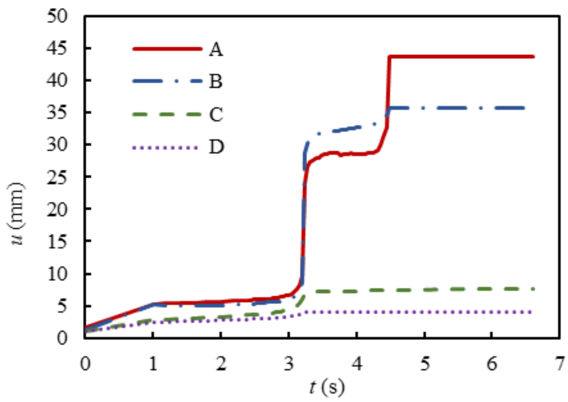

(a)

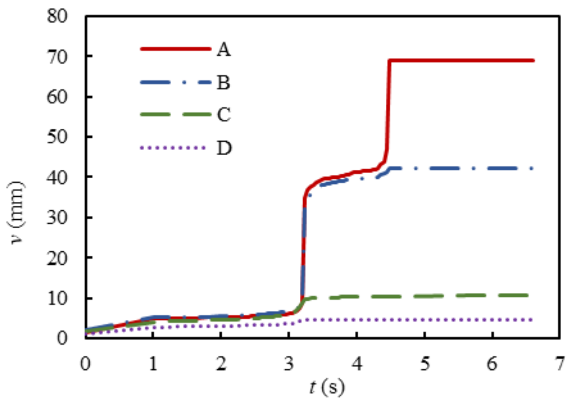

(b)

Figure 6. Displacement of typical points at the fifth excavation step in the dual structure slope; t, time after the last excavation step. (a) u, horizontal displacement; (b) v, vertical displacement.

In the dual structure slope, the displacement development of points located between the two slip surfaces during the fifth excavation step exhibits a markedly different pattern from that of the points above the shallower slip surface. These inner points experience only a brief and limited increase in displacement, followed by rapid stagnation. This contrast shows that the inner region near the deeper slip surface does not accumulate sufficient deformation to progress toward failure, whereas the outer region undergoes substantially larger and sustained deformation, ultimately controlling the initiation of slope failure.

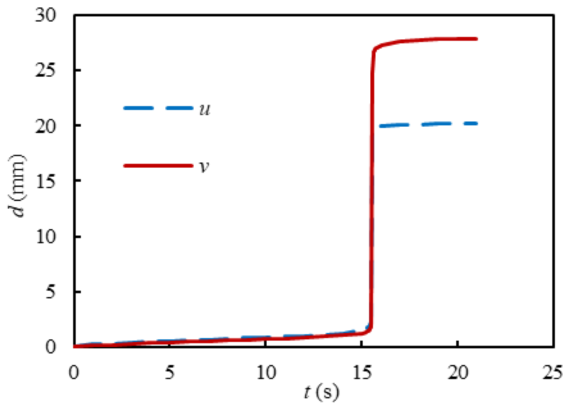

Figure 7. Displacement of point E in the pure clay slope at the fourth excavation step; u, horizontal displacement; v, vertical displacement; d, displacement; t, time after the last excavation step.

4 FAILURE MECHANISM

4.1 Failure mechanism analysis

For each slope, a representative elevation intersecting the sliding zone is selected, and the displacements of points along this elevation are monitored throughout the excavation process. Figure 8 illustrates the evolution of the horizontal displacement distribution at these typical heights.

The horizontal displacement along the height remains small before the final excavation step and increases to varying degrees afterward. In the inner regions of both slopes, horizontal displacement remains limited after the last excavation, whereas the outer regions exhibit pronounced displacement growth and significantly larger values. Due to these uneven growth rates, inflection points appear in the displacement distribution curves—two in the dual structure slope and one in the pure clay slope. Each inflection point marks the location where horizontal displacement becomes markedly greater than that of the inner portion. Close analysis shows that the locations of the reflection points are where the slip surfaces generate, suggesting that slope failure is closely related to the nonuniform displacement development.

And in the dual structure slope, although there is some increment of displacement between the two slip surfaces, it is much smaller than that in the region outside the shallower slip surface. This corroborates that only the outer part of the slope undergoes substantial deformation accumulation, while the inner part remains largely restrained, providing spacial evidence that the ultimate failure localizes along the shallower slip surface rather than the deeper one.

Additionally, at an excavation depth of 120 mm, the horizontal displacement in the dual structure slope remains very small, whereas the pure clay slope shows a larger initial displacement and continues to grow. This demonstrates that the dual-structure slope undergoes slower displacement development, leading to failure at a greater excavation depth.

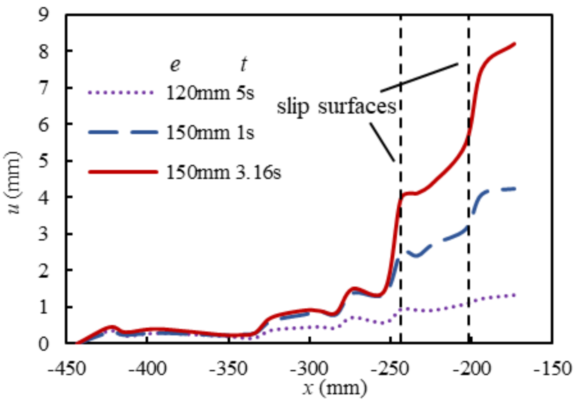

(a)

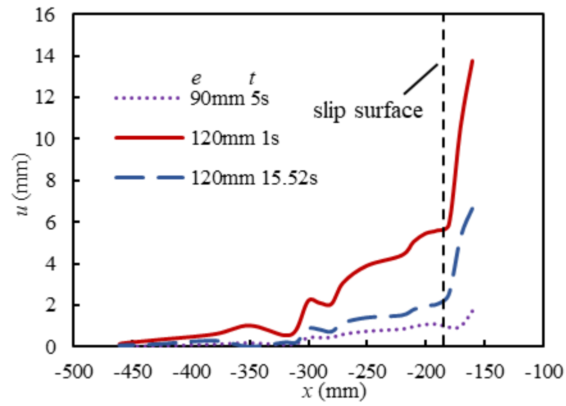

(b)

Figure 8. Horizontal displacement distribution development in typical height before failure; u, horizontal displacement; x, horizontal coordinate; e, excavation depth; t, time after excavation. (a) dual slope, y=113mm, landslides at e=150mm, t=3.16s; (b) pure clay slope, y=128mm, landslides at e=120mm, t=15.56s.

To furtherly investigate the relationship between uneven displacement development and slope failure, maximum shear strain is used as an indicator. It is calculated using square elements with side length of 10mm whose node displacement is measured and used for calculating.

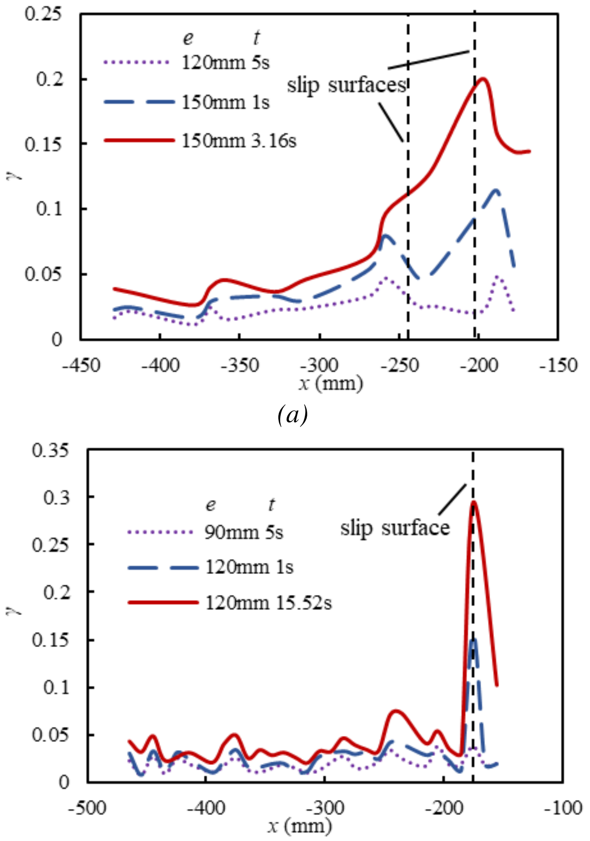

(a)

(b)

Figure 9. Development of maximum shear strain horizontal distribution along typical height before failure; γ, maximum shear strain; u, horizontal displacement; e, excavation depth; t, time after excavation. (a) dual slope, y=113mm, landslides at e=150mm, t=3.16s; (b) pure clay slope, y=128mm, landslides at e=120mm, t=15.56s.

Figure 9 shows the development of maximum shear strain horizontal distribution at the typical height crossing sliding part in each slope. In both slopes, the maximum shear strain develops as excavation deepen and time accumulating. Before the last excavation step, it is uniformly small. After the last excavation step, the maximum shear strain increases with various rate and becomes relatively large in certain places. Hence, there forms peaks on the distribution curve, indicating the gathering of particularly significant deformation localization. For both of the slopes, the peaks all coincidently locates at the places of the slip surfaces, meaning that the deformation localization leads to local failure and forms slip surfaces. Compare the initial peak generated curves with the subsequent ones, it can be seen that the maximum shear strain value around the peaks increases significantly and the peak range expands. The local failure promotes the deformation development in nearby area and lead to more significant deformation localization.

Hence, the failure mechanism for both the slopes can be explained as the coupling effect of deformation localization and local failure. The concentrated development of deformation forms deformation localization and leads to local failure. The occurrence of local failure makes the deformation localization become more intense and then results in further local failure. Under this positive feedback loop, the slope failure ultimately happens.

4.2 Failure mechanism application

The slope failure mechanism based on maximum shear strain development can be applicated in elaborating the influence of dual structure on slope failure patterns such as slip surface distribution and failure process.

The evolution of maximum shear strain horizontal distributions provides more direct evidence of how the dual structure affects failure surface forming. Unlike the pure-clay slope, two distinct strain-localization zones first appear at E = 150 mm and t = 1 s, and their peak positions coincide with the locations of the two slip surfaces. This indicates that deformation initially concentrates in two separate regions, each capable of initiating a potential slip surface. As excavation proceeds, the shear strain near both peaks intensifies, and by t = 3.16 s—immediately before final failure—the two peaks merge into a dominant localization zone, with its maximum value shifting toward the shallower slip surface. Meanwhile, deformation development near the deeper peak remains limited. As a result, the slope ultimately fails along the shallower slip surface, whereas the deeper potential slip surface stabilizes after only minor deformation. These observations demonstrate that the dual structure modifies the pattern of deformation localization and leads to differences in both pattern and final position of slip surfaces compared with the pure clay slope.

The time histories of maximum shear strain in the typical elements provide time insight into affection of dual structure on slope failure progress. These elements are selected at the locations corresponding to the peak values on curves immediately before failure in Figure 9. As shown in Figure 10(a), the maximum shear strain in each typical element increases slightly after every excavation step, yet the overall magnitude remains small. At all stages prior to failure, the typical element in the dual structure slope consistently exhibits smaller shear strain than that in the pure clay slope.

The two slopes also exhibit different deformation mood during the excavation step with failure (Figure 10(b)). In the pure clay slope, approximately 15 seconds after the fourth excavation step, the typical element shows a pronounced acceleration in maximum shear strain increment, forming a sharp inflection on its time-history curve. This inflection reflects the deformation localization accumulation threshold, beyond which failure becomes inevitable. Different, in the dual-structure slope, a comparable inflection appears only about 3 seconds after the fifth excavation step. And the final threshold shear strain at which this inflection occurs is even smaller than that in the pure clay slope before inflection.

These observations demonstrate that the dual structure modifies the deformation development process: it delays the accumulation of deformation, thereby postponing the onset of failure and enhancing the slope's excavation resistance. However, it also lowers the shear-strain threshold required to trigger local failure, indicating a reduced capacity of the slope to withstand concentrated deformation.

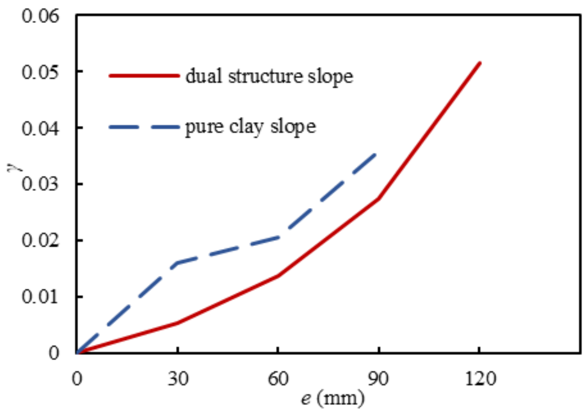

(a)

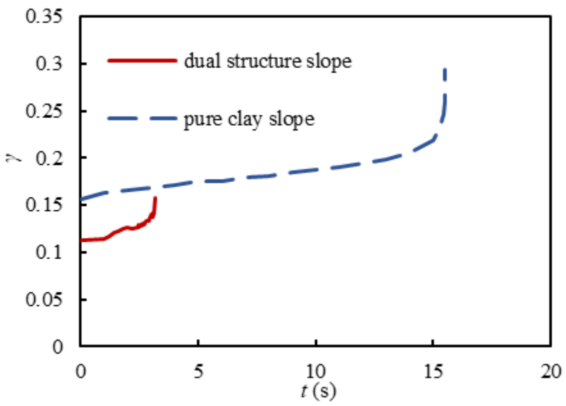

(b)

Figure 10. Maximum shear strain development during gradual excavation in typical elements; γ, maximum shear strain. (a) maximum shear strain caused by excavations steps before the failuer, e, excavation depth; (b) time history of maximum shear strain development during the last excavationt step, t, time after the last excavation step.

5 CONCLUSIONS

This study investigates the failure mechanism of dual structure slopes under gradual excavation condition through centrifuge model tests. The main conclusions are as follows.

(1) The slopes both occur rapid failure in a similar range during gradual excavation. There forms two slip surfaces in the dual structure slope while one in the pure clay one.
(2) The failure mechanism for both of the slopes is the coupling effect of deformation localization and local failure. Deformation localization forms during excavation and leads to local failure. Local failure advances the development of deformation localization nearby.
(3) Dual structure changes the deformation distribution of slope and therefore makes difference in slip surface pattern and failure range.
(4) Dual structure also delays the deformation developing process, increases the slope's resistance against excavation but reduces its withstand towards deformation.

ACKNOWLEDGEMENTS

The study is funded by National Key R&D Program of China (No. 2023YFC3007001).

REFERENCES

Gao, X., Tian, W. P., Li, J., Qi, H., Zhang, Z. and Li, S. (2022). Force and deformation response analysis of dual structure slope excavation and support. *Geomatics, Natural Hazards and Risk*, *13*(1), 501-537. https://doi.org/10.1080/19475705.2022.2037738

Huang, H., Zhao, J., Liu, S. and Ke, H. (2023). Centrifuge model test study on the mutual effect of water level variation and excavation on the deformation and failure of slopes. *KSCE Journal of Civil Engineering*, *27*(2), 521-534. https://doi.org/10.1007/s12205-022-2082-1

Li, M., Zhang, G., Zhang, J. M. and Lee, C. F. (2011). Centrifuge model tests on a cohesive soil slope under excavation conditions. *Soils and foundations*, 51(5), 801-812. https://doi.org/10.3208/sandf.51.801

Liu, S., Zhang, G. and Wang, A. (2024). Centrifuge model test study of structuralized cemented slopes under excavation conditions. *International Journal of Geomechanics*, *24*(3), 04024006. https://doi.org/10.1061/IJGNAI.GMENG-9205

Paudyal, P., Dahal, P., Bhandari, P. and Dahal, B. K. (2023). Sustainable rural infrastructure: guidelines for roadside slope excavation. *Geoenvironmental Disasters*, 10(1), 11. https://doi.org/10.1186/s40677-023-00240-x

Yang, Y., Sun, Y., Sun, G. and Zheng, H. (2019). Sequential excavation analysis of soil-rock-mixture slopes using an improved numerical manifold method with multiple layers of mathematical cover systems. *Engineering Geology*, 261, 105278. https://doi.org/10.1016/j.enggeo.2019.105278

Zhang, G., Hu, Y. and Zhang, J. M. (2009). New image analysis-based displacement-measurement system for geotechnical centrifuge modeling tests. *Measurement*, 42(1), 87-96. https://doi.org/10.1016/j.measurement.2008.04.002

Zhang, F., Liu, G., Chen, W., Liang, S., Chen, R. and Han, W. (2012). Human-induced landslide on a high cut slope: a case of repeated failures due to multi-excavation. *Journal of Rock Mechanics and Geotechnical Engineering*, 4(4), 367-374. https://doi.org/10.3724/SP.J.1235.2012.00367

Zhang, Q., Wang, J., Wang, W., Bai, S. and Lin, P. (2019). Study on slope stability due to the influence of excavation of the high-speed rail tunnel. *Geomatics, Natural Hazards and Risk*. https://doi.org/10.1080/19475705.2019.1568311

Zhang, S., Pei, X., Wang, S., Huang, R. and Zhang, X. (2020). Centrifuge model testing of loess landslides induced by excavation in Northwest China. *International journal of geomechanics*, 20(4), 04020022. https://doi.org/10.1061/(ASCE)GM.1943-5622.0001619